Influence of Flow in The Adhesion and Proliferation of Cells on Hydroxyapatite Integrated in a Microscale Culture

A.R. Atif[1], M. Pujari-Palmer[1], M. Tenje[1], G. Mestres[1]

[1]*Dept. Materials Science and Engineering, Science for Life Laboratory, Uppsala University, Uppsala, SE*

INTRODUCTION: Synthetic biomaterials, such as calcium phosphate cements (CPCs), are a promising alternative to autologous bone to enhance bone regeneration. Calcium-deficient hydroxyapatite (CDHA), the end-product of apatite cements, matches the inorganic phase of the bone and exhibits excellent biocompatibility *in vivo* [1]. However, *in vitro*, CDHA uptakes calcium ions (Ca^{2+}) from cell culture medium [2], causing detrimental effects on cell activity and function [3]. The aim of this work was to integrate CDHA into a microfluidic chip that provides continued culture medium supply, and to evaluate cell adhesion and proliferation as compared to standard well plates.

METHODS: CDHA was integrated in a polydimethylsiloxane (PDMS)-glass microfluidic chip (CDHA-on-chip). PDMS was cured in a 3D-printed mould at 60°C for 2h. α-tricalcium phosphate was mixed with 2.5% w/v $Na_2HPO_{4(aq)}$ (liquid-to-powder of 0.65 ml/g) and the CPC was cast within a PDMS pocket. The CPC was immersed in an aqueous solution at 37°C for 10 days to ensure full transformation to CDHA. Through plasma treatment, a glass slide was bonded to the PDMS holding the CDHA, thus forming a 0.5mm channel above the CDHA. CDHA samples were pre-incubated for 24h in minimum essential media (MEM) supplemented with 10% FBS and 1% penicillin-streptomycin (sMEM). Pre-osteoblasts (MC3T3-E1) were seeded at 50,000 cells/cm^2 and after a cell adhesion period of 2h, flow was applied for 72h through the chip at different rates: 2, 8 and 14 µl/min. A static (0 µl/min) chip condition was included, where sMEM was manually replaced every 24h. CDHA discs (⌀=6mm, h=2mm) placed in a 96-well plate were used as a standard static control (200 µl sMEM replaced every 24h). At 6h and 72h, the cells were stained with a calcein, propidium iodide and Hoechst triple-stain to assess their adhesion and proliferation, respectively. In a separate experiment, sMEM was flown through the chips for 24h at the aforementioned flow rates, and Ca^{2+} concentration was quantified via inductively coupled plasma-optical emission spectroscopy (ICP-OES). As control, sMEM in contact with CDHA discs for 24h was evaluated.

RESULTS: A larger number of cells adhered on the CDHA-on-chip under flow as opposed to both static CDHA-on-chip and CDHA disc in a well plate. Differences in cell adhesion between the flow conditions were negligible. Cell proliferation at 72h was significantly increased under flow compared to CDHA disc samples (Fig.1A). Static CDHA-on-chip showed almost no viable cells. 2 and 8 µl/min flow conditions showed the greatest cell counts, followed by the 14 µl/min flow condition. At higher flow rates, Ca^{2+} concentrations were closer to in fresh medium (Fig.1B).

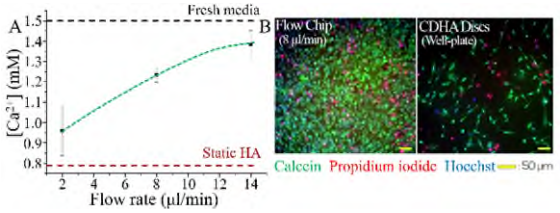

Fig. 1: A) Calcium concentration in sMEM. B) Stained cells after 72 h of culture.

DISCUSSION & CONCLUSIONS: The static CDHA-on-chip and disc samples displayed a low degree of cell adhesion and proliferation, which seemed to indicate that ionic exchange led to detrimental cell behaviour. Cells displayed the greatest degree of adhesion and proliferation at a flow rate of 2 and 8 µl/min, probably due to more optimal Ca^{2+} concentrations. At 14 µl/min, the degree of cell adhesion and proliferation decreased, which could be ascribed to adverse effects of shear stress.

ACKNOWLEDGEMENTS: G. Mestres acknowledges Formas (2016-00781) and VR (2017-05051), and Göran Gustafsson's Foundation (1841) for financial support.

REFERENCES: [1] Ginebra, MP. EFORT Open Rev. 3 (2018) 173–183. [2] Gustavsson, J. et al. Acta Biomater. 7, 4242–4252 (2011); [3] Sadowska, JM et al. Tissue Eng. A 23 (2017) 1297-1309.

Novel Sodium Alginate - Hydroxyapatite Nanoparticles Bilayer Membranes: Synthesis and Characterization

N. D'Elía[1], R. Rial Silva[2], J. Sartuqui[1], D. Ercoli[3], J. Ruso[2], P. Messina[1], G. Mestres[4]

[1]Chemistry Dept, Universidad Nacional del Sur, INQUISUR-CONICET, Bahía Blanca, AR, [2]Soft Matter and Molecular Biophysics Group, Santiago de Compostela University, Santiago de Compostela, ES, [3]Chemical Engineering Pilot Plant - PLAPIQUI-UNS-CONICET, Bahía Blanca, AR, [4]Engineering Sciences Dept., SciLifeLab, Uppsala University, Uppsala, SE

INTRODUCTION: Guided bone regeneration consists in covering a bone defect with a membrane that acts as a barrier (from rapidly growing epithelium) in order to support both the growth of osteoblasts and wound healing [1]. Alginate (ALG) is widely used in biomedical applications due to its clinical biocompatibility, and hydroxyapatite nanoparticles (HAn) stimulate osteoblast differentiation [2]. The main goal of this work was to develop a novel ALG-HAn bifunctional membrane capable of stimulating bone formation on one side and wound healing on the other.

METHODS: The membranes were obtained following a modified synthesis of Benedini et al. [3]. A side of the ALG membranes, namely mineral side (MS), was crosslinked with a solution containing HAn (0.11, 0.55 and 1.1 wt%) and 110 mM $CaCl_2$. On the other side, namely fibrous side (FS), ALG was crosslinked with a solution containing only $CaCl_2$. Membranes completely free of HAn were used as control (0 wt%). The ALG-HAn interaction was evaluated with Fourier-transform infrared spectroscopy (FTIR) and the hydrogels viscosity by rheology. The membranes were visualized by scanning electron microscopy (SEM) and tested by tensile assays. Their degradation was evaluated by immersion in phosphate buffer solution (PBS) at 37 °C over 7 days. Finally, the proliferation of fibroblasts (hDF) and osteoblasts (Saos-2) on the FS and MS, respectively, was tested by PrestoBlue assays. Osteoblastic differentiation was studied by alkaline phosphatase activity (ALP).

RESULTS: The FTIR spectrum of the membranes showed a shift of the COO^- group bands attributed to the ionic bonding between ALG and HAn. The ALG-HAn interaction had a clear effect in the increase of hydrogels viscosity. In addition, the amount of HAn concentration was inversely proportional to the plasticity and Young modulus of the membranes. In contrast, the degradation of the membranes increased with a higher amount of HAn. The membranes FS showed a heterogeneous porosity (ø = 65.9 ± 28 µm), whereas the MS had lower porosity and a heterogeneous presence of HA microaggregates. Both fibroblasts (cultured on FS) and osteoblasts (cultured on MS) proliferated over time on all membranes tested. The osteoblasts differentiation was directly proportional to the HAn amount present (Fig. 1).

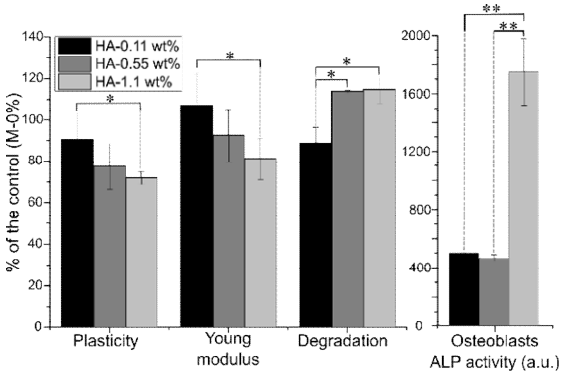

Fig. 1: Properties of the membranes.

DISCUSSION & CONCLUSIONS: Bifunctional membranes with bilayer surface characteristics were obtained being a promising material for guided bone regeneration applications.

ACKNOWLEDGEMENTS: The authors thank Stint (GM, # IB2017-7362), CONICET (ND and JS postdoctoral fellowships), UNS (PGI 24 / Q064), Ramón Areces Foundation and Xunta de Galicia (ED41E2018/08) for financing this project.

REFERENCES: [1] Dimitriou R. et al. BMC Medicine 10 (2012) 81. [2] D'Elía N.L. et al. Biochim. Biophys. Acta – Gen. Subj. 1830 (2013) 5014. [3] Benedini L. et al. Colloid. Polym. Sci. 295 (2017) 2109.

Properties and Dynamics Behaviour of Novel Antibacterial Hydrogel Coatings for Implants

M. Gasik[1], A. Zühlke[1], V. Gribova[2], P. Lavalle[2], N. E. Vrana[3]

[1]Aalto University Foundation, Espoo, FI, [2] INSERM, Strasbourg, FR, [3] Spartha Medical SAS, Strasbourg, FR

INTRODUCTION: Persistent antibiotic resistance of pathogens is a growing healthcare concern. Complications are observed for many biomaterials due to biofilm formation, which conventional treatment is difficult.
Here we present the novel type of antibiotic-free coating having intrinsic antibacterial ability without cellular toxicity and improved biomechanical properties.

METHODS: Novel coatings were made with hyaluronic acid (HA) of <1 MDa molecular weight, cross-linked with 10-20% BDDE under optimized technology for coatings of 50-2000 µm thickness. Stand-alone hydrogel specimens of ~1.5 x 5 mm diameter were made for mechanical testing. The antibacterial properties of the hydrogels were achieved with poly-arginine (PAR), introduced into the gels in different quantities. The antibacterial functionality of new HA-PAR hydrogels was tested on *S. aureus* culture.
Stand-alone specimens were evaluated on their biomechanical properties with dynamic mechanical analysis (DMA) under physiological conditions (37°C) at pseudo-static and dynamic (1 Hz) loading in DMEM media, mimicking exerted soft tissues pressure of 4-6 kPa. Elution of PAR under static and dynamic conditions was assessed by fluorescent spectrophotometry and Raman spectroscopy.

RESULTS: Experimental results show excellent antibacterial properties of novel coatings using optimal PAR composition, also well retained after autoclaving.
Biomechanical tests have demonstrated HA-PAR gels being stiffer under creep conditions (slope modulus 50-120 kPa at 4-7 kPa constant applied stress) vs. pure HA gels (20-60 kPa), Fig. 1. This difference was more pronounced under dynamic conditions: 45-50 kPa for HA-PAR at 1 Hz vs. 15-30 kPa for HA gels (applied stress amplitude 3-6 kPa; statistical data not shown here).

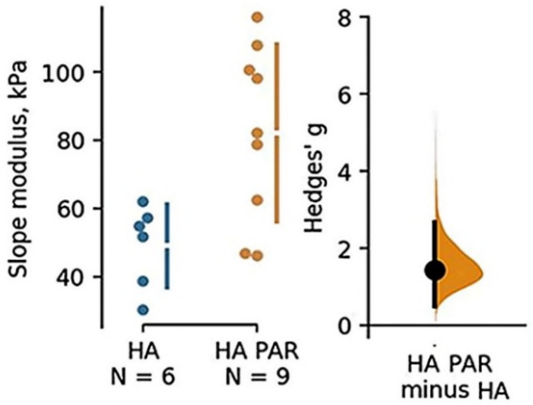

Fig. 1: Slope modulus of HA and HA-PAR gels under different stresses (Hedges' g-value (effect size) = 1.43; Mann-Whitney test p=0.0290).

PAR release under dynamic loading, determined by Raman spectroscopy, was substantially higher than in static conditions, which suggests that coated implants expecting to bear more dynamic loading might need different PAR composition and concentration than ones working in more static cases.

DISCUSSION & CONCLUSIONS: Optimal chain length PAR with a proper HA cross-linked gel coatings were demonstrated superior antibacterial activity with no evident cytotoxicity. PAR-laden gels were determined also to have higher PAR release under dynamic mechanical loads, exhibiting also higher stiffness.

ACKNOWLEDGEMENTS: This project has received funding from the European Union's Horizon 2020 research and innovation programme under grant agreement No 760921 "PANBioRA" (www.panbiora.eu).

3D Printing of Polyetheretherketone/Hydroxyapatite Composite Materials for Orthopaedic Implant Applications

A.R. Boyd[1], K.P. Rodzen[1], L. Stipniece[2], K. Salma-Ancane[2], J.A. Acheson[1], M.J. Morton[1], A. McIlhagger[1] and B.J. Meenan[1]

[1]Nanotehnology and Integrated Bioengineering Centre, School of Engineering, Ulster University, UK, [2] Rudolfs Cimdins Riga Biomaterials Innovations and Development Centre, Riga Technical University, LV

INTRODUCTION: Polyetheretherketone (PEEK) is a high-performance thermoplastic polymer which has found increasing application in orthopaedic implant devices and has shown a lot of promise for 'made-to-measure' implants produced through additive manufacturing approaches [1]. However, a key limitation of PEEK is that it is bioinert. There is therefore a need to provide a mechanism to functionalise its surface to make the material at least osteoconductive to ensure a more rapid, improved and stable fixation that will last longer, *in vivo*. One approach to solving this issue is to modify PEEK with bioactive calcium phosphate (CaP) materials, such as hydroxyapatite (HA). The work reported in this study will demonstrate the creation of a PEEK/HA composite filament, which is subsequently 3D printed using a Fused Filament Fabrication (FFF) approach. The mechanical, chemical, physical and in vitro properties of the composite materials was investigated.

METHODS: Filaments of PEEK/HA composite (1.75 mm in diameter) with up to 30% w/w HA/PEEK were manufactured using a continuous twin-screw extrusion process. The filaments were subsequently 3D printed into test samples using a modified version of commercial FDM printer suitable for use with Advanced Composite Materials. The samples were characterized using Dynamic Mechanical Analysis (DMA), tensile testing, Thermogravimetric Analysis (TGA), X-Ray Diffraction (XRD), Scanning Electron Microscopy and Energy Dispersive X-Ray Analysis (SEM/EDX), X-Ray Photoelectron Spectroscopy and Computed Tomography (CT) scanning methods.

RESULTS AND DISCUSSION: The CT images of both the filament and the 3D printed samples showed that the HA material was evenly dispersed throughout the bulk all the samples. SEM and EDX measurements highlighted that on the surface of the samples, hydroxyapatite could be easily observed, and were homogenously distributed across the surface of all the samples produced. EDX mapping conformed this. XPS measurements of the surface showed the presence of Ca and P in the uppermost surface regions (5-10 nm) of the HA/Composite materials. The corresponding XRD data clearly showed the presence of crystalline HA in each HA/PEEK sample, matching the expected peaks for International Centre for Diffraction Data (ICDD) file #09-0432 for HA. As the HA content of the samples increases, so does the tensile modulus, ranging from 4.2 GPa (PEEK) to 6.1 GPa (30% HA/PEEK) and are significantly higher than datasheet information of injected molded PEEK samples. That is due to a higher degree of crystallinity obtained during 3D printing compared to injection molded samples, where specimens are cooled quickly in the mold.

CONCLUSIONS: In conclusion, the results clearly show that we can successfully 3D print HA/PEEK composite materials up to 30% w/w HA/PEEK. The samples produced have a homogeneous distribution of HA in both the bulk and surface of all the samples, and their mechanical performance of the PEEK is not significantly affected by the addition of HA. As such, the methodology outlined here provides a route to easily manufacture bioactive HA/PEEK composites for orthopaedic applications.

ACKNOWLEDGEMENTS: The North West Centre for Advanced Manufacturing (NW CAM) project is supported by the European Union's INTERREG VA Programme, managed by the Special EU Programmes Body (SEUPB). The views and opinions in this document do not necessarily reflect those of the European Commission or the Special EU Programmes Body (SEUPB).

REFERENCES: [1] A Haleem and M Javaid. Clin Epidem Global Health. (2019) In Press.

Alignment of Carbon Nanotubes Into Gellan Gum Hydrogel Matrices via Magnetic Field

M. Saranya[1], J.T. Kovisto[1], L. Janssen[1], O. Pitkänen[1], T. Järvinen[1], M. Kellomäki[2], K. Kordas[1] and G.S. Lorite[1]

[1]Microelectronics Research Unit, University of Oulu, FI, [2] Biomaterials & Tissue Engineering Group, BioMediTech, Faculty of Medicine and Health Technology, Tampere University, FI

INTRODUCTION: The use of nanomaterials as an active component in 3D matrices have recently gained attention to stimulate and induce cell growth and tissue regeneration. Hydrogels have been used as strategy to create 3D matrices to enable tissue repairing. However, hydrogels typically lack to mimic the extracellular matrix (ECM). In addition, to induce cell growth in specific orientation is crucial in various tissues like the cardiac muscle, neurons and cartilages [1]. In our previous work, we have demonstrated the use of carbon nanotube (CNT) micropillared template to align neuron [2] and chondrocytes [3] growth. Our current work focuses on how to transfer these results to 3D matrices. Previous report has shown CNTs alignment in hydrogel by electric field, which requires electrodes limiting the clinical applicability [4]. Here, we demonstrate the integration and alignment of multi walled CNTs (MWCNTs) into gellan gum (GG) hydrogel by using magnetic field.

METHODS: MWCNTs were grown on silicon substrate by catalytic (ferrocene) chemical vapor deposition in a quartz tube reactor. The MWCNTs obtained were functionalized with carboxylic acid in an acid mixture enabling homogenous dispersion in sterile water with concentration ranging from 0.01 to 0.2 mg/mL. The pristine GG were prepared in sucrose solution. Mixing of GG with varied concentration of MWCNT-COOH solution (MWCNT/GG) was performed at 90 °C. The hybrid hydrogels were crosslinked with spermine tetrahydrochloride (SPM). The alignment is achieved by applying magnetic field (600 mT). The MWCNT-COOH were characterized by means of TEM, EDS, Raman and the hybrid hydrogels in terms of compression and rheology tests.

RESULTS: The average outer diameter of MWCNT-COOH was found to be 26 nm (via TEM). EDS analysis shows the presence of carbon, oxygen and iron as expected. The Young's modulus of MWCNT/GG increases with increase in concentration of MWCNT in GG. Rheologically, storage modulus shows the same trend while the loss modulus decreases with increase in MWCNT concentration showing elastic behaviour dominates over viscous behaviour. The alignment of MWCNT into GG by applying magnetic field is confirmed via optical measurement setup, which displayed maximum transmittance when laser polarization plan field E is perpendicular and minimum when it is parallel (Fig 1). The pristine GG did not alignment.

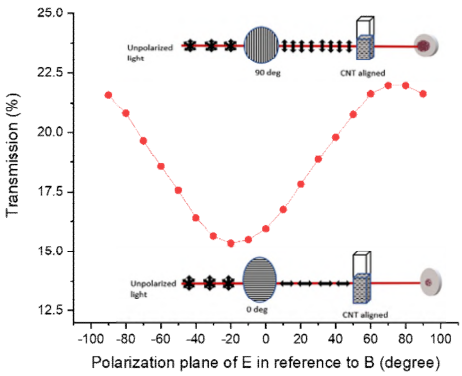

Fig. 1: Alignment of MWCNT into GG using magnetic field of 600mT at room temperature.

DISCUSSION & CONCLUSIONS: We have successfully demonstrated the alignment of MWCNT-COOH into hydrogel matrix via magnetic field. The method proposed here is less invasive method to align MWCNT in hydrogels, broadening the possibilities in tissue engineering at clinical level.

ACKNOWLEDGEMENTS: This work was funded by Academy of Finland (#317437 and #320090).

REFERENCES: [1]Y. Li *et al.*, *Bio. Adv.*, 2014. [2] G. S. Lorite *et al.*, *Nano Res.*, 2019, [3] L. Janssen *et al.*,*Carbon* ,2019, [4] S. Ahadian *et al.*, *Sci. Rep.*, 2014.

Strontium Ion Containing Amorphous Calcium Phosphate

J. Vecstaudza[1], K. Katkovska[1], J. Locs[1,2]

[1]Rudolfs Cimdins Riga Biomaterials Innovations and Development Centre of RTU, Institute of General Chemical Engineering, Faculty of Materials Science and Applied Chemistry, Riga Technical University, Riga, LV, [2]Baltic Biomaterials Centre of Excellence, Headquarters at Riga Technical University, Riga, LV

INTRODUCTION: Osteoarthritis (OA) is the most common type of arthritis, that can affect any joint. OA can disrupt both joint's cartilage and subchondral bone and can cause inflammation. Sr ranelate has positive effect on subchondral bone and cartilage tissues affected by OA [1]. However, intake of Sr ranelate has been associated with adverse health effects, therefore other ways of Sr administration are needed. Therefore, local delivery of Sr through dissolution of Sr containing calcium phosphate nanoparticles in the joint areas for subchondral bone regeneration could be a progressive and novel solution. Aim of the study was to synthesize and investigate Sr containing ACP nanoparticles with different Sr concentrations.

METHODS: Synthesis of ACP [2] was specifically modified to obtain Sr-ACP. The modification included addition of Sr containing salt to the synthesis medium. At first calcium and phosphate ion rich solution was prepared by dissolving hydroxyapatite in HCl, then Sr containing salt was added. Precipitation from this solution was done by rapid rise of pH up to 11 by adding NaOH solution under intense stirring. Sr-ACP was washed with deionized water and dried at 70-90 °C. Phase composition was checked with XRD, chemical groups were detected with FT-IR, chemical composition was determined with SEM-EDS and specific surface area (SSA) was measured with BET N_2 adsorption technique. Amorphous phase stability test for ACP and Sr-ACP in water at 22 °C and 37 °C was done as well.

RESULTS: XRD patterns revealed that all synthesized samples were amorphous. In addition to the information about samples being amorphous FT-IR spectra confirmed presence of hydrated layer and carbonate ions. The amount of introduced Sr into the structure of ACP and value of SSA is shown on Table 1. Amorphous phase stability test proved that Sr-ACP synthesized by the developed technology remained stable for at least 2 hours at 22 °C and 37 °C.

Table 1. Theoretical and experimental Sr/[Sr+Ca] molar ratios and SSA of Sr-ACP.

Theoretical Sr/[Sr+Ca]	Experimental Sr/[Sr+Ca]	SSA, m^2/g
0.22	0.18	176
0.74	0.50	144

DISCUSSION & CONCLUSIONS: Sr ions preserved the structure of ACP synthesized by the method developed by our group previously [2]. As SSA of the Sr-ACP samples was high – well above 100 m^2/g it fitted nicely into range of SSA values of bone mineral particles (80-240 m^2/g [3]). Less of Sr ions were included into Sr-ACP than were added in the synthesis solution. That is a common trend in synthesis of ion substituted calcium phosphates. Overall, the synthesis of Sr-ACP proved to be successful in tested Sr concentration ranges. The carbonation (observed in FT-IR) and high SSA assures the similarity to bone mineral phase. Further, the good solubility and biocompatibility of ACP itself gives a promising future for Sr-ACP to be used in treatment of the bone defects. It would stimulate bone regeneration and contribute to other biological processes, where Sr is involved.

ACKNOWLEDGEMENTS: EuroNanoMed[3]: "Nanostructured Osteochondral Scaffold: Novel Biomimetic Triggers for Enchanced Bone Regeneration", Nano-Scores, 2018-2021.

REFERENCES: 1. Z. Huang, C. Ding, T. Li, et al. Rheumatology (United Kingdom), 57 (2018), iv108-iv123. 2. J. Vecstaudza, J. Locs, J. Alloy. Compd., 700 (2016), 215-222. 3. J. Kolmas, A. Ślósarczyk, A. Wojtowicz, et al. Solid State Nucl. Mag., 32 (2007), 53-58.

Enhanced Cellular Functions on Nanophase Tantalum Oxide Surfaces

E. Uslu[1], S. Odabaş[2], B. Ercan[1,3]

[1]Department of Metallurgical and Materials Engineering, Middle East Technical University, Ankara, TR, [2]Ankara University, Faculty of Science, Department of Chemistry, Ankara, Turkey [3]BIOMATEN, Middle East Technical University, Center of Excellence in Biomaterials and Tissue Engineering, Ankara, TR

INTRODUCTION: Being among valve metals, tantalum forms a naturally occurring stable oxide layer on its surfaces under oxidizing conditions. This stable oxide layer prevents corrosion and makes tantalum chemically inert. Moreover, tantalum offers optimal mechanical properties to be used in orthopaedic applications. Thus, it is considered as one of the next generation metals for orthopaedic implants. However, the bioinert nature of tantalum surface hinders its osseointegration with juxtaposed tissue. As a remedy, tantalum surfaces can be modified at the nanoscale via anodization. Anodization is an electrochemical process to grow the naturally occurring oxide layer where size and morphology of the surface features can be altered to enhance biological functions.

METHODS: Concentrated HF:H_2SO_4, DMSO and NH_4F were used as electrolytes in an electrochemical cell. Anodization duration (1 min-2.5 h) and applied potential (10V-60V) were fine-tuned to obtain nanotubular, nanocoral and nanodimple surfaces. Adhesion and proliferation of human osteoblast cells and adipose tissue-derived mesenchymal stem cells (MSC) were examined up to 5 days *in vitro*. RT-PCR experiments were conducted to observe gene expressions of mesenchymal stem cells using 5 different genes (ALP, Osteonectin, Osteocalcin, Collagen I, Collagen II) up to 3 weeks.

RESULTS: Concentrated HF: H_2SO_4 solution were used to obtain nanotubular morphology. Applied potentials were altered from 10V to 55V to control feature size of the nanotubes between 15 to 150 nm. Nanocoral tantalum surfaces were obtained by using 3.3 wt% NH_4F in 1M H_2SO_4 solution. In this morphology, durations were fine-tuned between 60 to 150 min and doing so, nanocoral feature sizes ranging between 20 to 120 nm were obtained. 5 vol% DMSO in concentrated HF: H_2SO_4 solution were used as electrolyte to obtain nanodimple morphology. Dimple size increased from 25 nm to 90 nm by changing voltage (10-35V) and anodization duration (10-30 min). Both osteoblasts and MSCs adhered more on anodized tantalum compared to non-anodized tantalum at 4 hr. Osteoblast and MSCs also proliferated more on anodized tantalum compared to non-anodized tantalum up to 5 days *in vitro*, while nanodimple surfaces supported the highest cell density at 5 days. In addition, osteogenic differentiation of MSCs upregulated upon the anodization of the surfaces to obtain nanophase surface features.

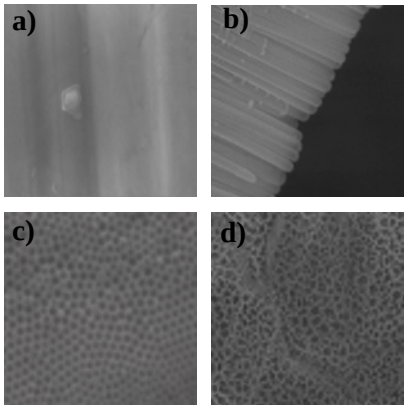

Fig. 1: a) Non-anodized, b) nanotubular, c) nanodimple and d) nanocoral surface morphologies of anodized tantalum.

DISCUSSION & CONCLUSIONS: Three different morphologies were obtained via anodization on tantalum surfaces with feature size altering between 15 to 150 nm. Osteoblast and MSC adhesion, proliferation and differentiation were enhanced *in vitro*. Thus, anodization of tantalum surfaces to obtain nanofeatures was considered to be a promising tool for orthopaedic applications.

ACKNOWLEDGEMENTS: Authors would like to thank the Scientific and Technological Research Council of Turkey (Grant no: 117M187) and BAGEP for providing financial support.

Production and Characterization of Catheters Capable of Resisting Device Associated Infection

B. Shaqour[1], A. Vazquez-Rodriguez[2], C. Guarch Pérez[3], J. Aizawa[1], E. Choińska[4], M. Riool[3], B. Verleije[5], K. Beyers[5], L. Ferrari[2], A. Felici[2], S. A. J. Zaat[3], W. Święszkowski[4], P. Cos[1]

[1]Antwerp University, BE, [2]Aptuit (Verona) Srl, an Evotec Company, IT, [3]Amsterdam UMC, NL, [4]Warsaw University of Technology, PL, [5]Voxdale bv, BE

INTRODUCTION: Device associated infection (DAI) is considered one of the greatest challenges in the medical field which affects around 700,000 patients annually in the U.S. alone[1]. The wide use of antibiotics to treat DAI causes rapid development of resistant pathogens, necessitating the search for alternative drugs to prevent or treat DAI. As the process for drugs discovery and pursuing authorities' approval is very expensive and time-consuming, the trend for repurposing already approved drugs is promising. Niclosamide (NIC) is an FDA approved anthelmintic and molluscicide drug that showed antibacterial and antibiofilm capabilities against species such as *Staphylococcus (S.) aureus*[2]. This study aimed at producing catheters loaded with NIC and investigating their properties.

METHODS: Thermoplastic polyurethane (TPU) catheters and fibres were hot melt extruded using a single screw extruder setup fitted with a special nozzle at 180°C. Films of TPU only and loaded with NIC were prepared by the solvent casting method using Chloroform as a solvent. NIC was loaded into the polymeric matrix at three ratios: 2%, 5% and 10% (w/w). The thermal and mechanical properties of the fibres were evaluated using a thermogravimetric analyser (TGA) and a tensile testing machine, respectively. Additionally, the release and antibacterial activity of the catheters were assessed *in vitro* against *S. aureus (ATCC 25923)* and *S. epidermidis (O-47)*.

RESULTS: TGA analysis showed that NIC degradation occurs at temperature above 220°C. The NIC was homogeneously distributed in the films as no agglomerates were observed after casting. Fibres with a diameter of around 0.8 mm and catheters with inner and outer diameter of 0.7 mm and 1.2 mm, respectively, were successfully produced. The mechanical properties of the produced fibres showed no statistical difference in the elastic modulus except with drug loading of 10% (w/w). Drug release tests showed a burst release up to 96 hours followed by a sustained release over the following period of test. Around 90% of the loaded drug was released from samples loaded with 2% and 5% of NIC (w/w), while, around 80% was released from samples loaded with 10% (w/w). The Kirby Bauer antimicrobial activity assay showed that the loaded catheters were active against the two tested bacterial species for the whole duration of the test (10 days).

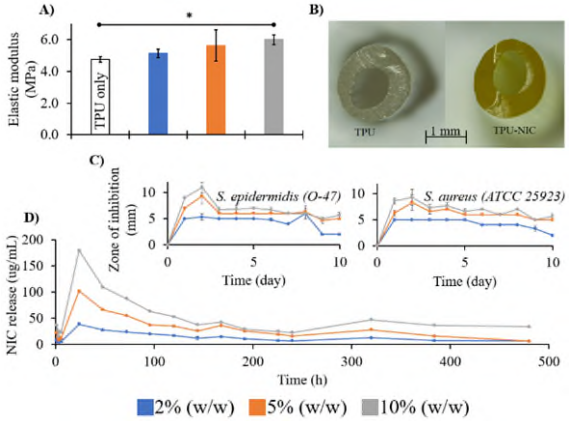

Fig. 1: Elastic modulus of produced fibres (A), Produced catheters (B), Zone of inhibition (C) and NIC release (D).

DISCUSSION & CONCLUSIONS: This study showed the feasibility of producing TPU catheter loaded with NIC using the hot melt extrusion process. Additionally, it shows that such catheters provide promising antibacterial properties.

ACKNOWLEDGEMENTS: This research was funded by the research project PRINTAID, the EU Framework Programme for Research and Innovation within Horizon 2020 - Marie Sklodowska-Curie Innovative Training Networks under grant agreement No. 722467.

REFERENCES:

1. Gwisai et al. (2017). Biomedical Materials, 12(4), 045010., 2. Zhurina et al. (2017). Microbiology, 86(4), 455-462.

Effect of Vitamin K2 and D in a Three-Dimensional *In vitro* Model of Primary Human Periodontal Ligament Fibroblasts

M. Schroeder[1], A. Eriksson Agger[1], J. He[2], B. H. Skallerud[2], H. J. Haugen[1], J. E. Reseland[1]

[1] University of Oslo, Department of Biomaterials, Institute of Clinical Dentistry, Oslo, NO, [2] Norwegian University of Science and Technology, Department of Structural Engineering, Faculty of Engineering, Trondheim, NO

INTRODUCTION: 3D *in vitro* models are of increasing interest for periodontal tissue engineering and the investigation of periodontal disease mechanisms or treatment options[1]. Fibroblasts residing within the periodontal ligament (PDL) are proposed to play a key role in the maintenance and repair of periodontal tissues[2]. Vitamin D functions in bone metabolism and mineral homeostasis but also plays crucial roles in modulation of the immune system and inflammatory responses[3]. Vitamin K2 has positive effects on bone formation and prevention of bone loss[4]. In this study, we generated spheroids from human primary periodontal ligament fibroblasts (hPDLFs) in a rotating bioreactor system that promotes cellular aggregation by slow horizontal clinorotation. The *in vitro* effect of vitamin K2 and D, both alone and combined, was tested on the mechanical properties of the hPDLF spheroids, as well as on proteins involved in the extracellular matrix (ECM) formation, osteogenic behavior, angiogenetic and inflammatory properties. Effects in the 3D cultures were compared to traditional 2D monolayer cultures.

METHODS: hPDLFs were cultures in 3D (BioArray Matrix drive BAM v4, CelVivo, Blommenslyst, Denmark) and 2D. Spheroids and 2D cultures were incubated with vitamin K2 and $25(OH)D_3$ or $1,25(OH)_2D_3$, alone and in combination. Cultures without vitamins were used as control. hPDLF spheroids were characterized in terms of their mechanical response by nanoindentation (Hysitron, Minneapolis, USA). Furthermore, ECM formation and mineralization, in both 3D and 2D cultures, were characterized by microscopy. The secretion of cytokines and bone factors to the culture medium was analysed applying multiplex immunoassays.

RESULTS: Mechanical testing revealed that both $25(OH)D_3$ alone, and in combination with K2, induced a softer or more flexible spheroid compared to the control. In line with that, significantly increased deposition of collagen type I was detected in frozen sections of hPDLF spheroids incubated with either vitamin K2 ($p < 0.01$) or K2 in combination with $25(OH)D_3$ ($p < 0.05$), while $25(OH)D_3$ alone enhanced the protein expression of periostin ($p < 0.01$). Moreover, we observed increased levels of interleukin-6 and alkaline phosphatase in the culture medium of the hPDLF spheroids, concomitant with a reduction of the release of DKK-1 and SOST. A beneficial effect of $25(OH)D_3$ on hPDLF osteogenic properties was also seen in the 2D cultures after 14 days, however, it was less prominent than in 3D.

DISCUSSION & CONCLUSIONS: Our results suggest that combined administration of vitamin D and K2 may be advantageous over single treatment with vitamin D in the regeneration of soft and hard tissue defects caused by periodontitis.

ACKNOWLEDGEMENTS: JE Reseland is a member of Cost action CA16119 CellFit.

REFERENCES:[1] Berahim Z, Moharamzadeh K, Jowett AK, Rawlinson A 2015, *Int J Dent*, 2015, 605813, [2] McCulloch CA, Bordin S 1991, *J Periodontal Res.*, 26, 144-54, [3] Colotta F, Jansson B, Bonelli F 2017, *J Autoimmun*, 85, 78-7, [4] Plaza SM, Lamson DW 2005, *Altern Med Rev*, 10, 24-35.

Mechanical and Structural Evaluation of Synthetic Trabecular Bone Models Printed with Stereolithography

A. Grzeszczak[1], S. Lewin[1], O. Eriksson[2], J. Kreuger[2], C. Persson[1]

[1]*Department of Materials Science and Engineering, Uppsala University, Uppsala, SE*
[2]*Department of Medical Cell Biology, Uppsala University, Uppsala, SE*

INTRODUCTION: Synthetic bone models are needed to train surgeons but also to test and design medical equipment. However, currently available models do not accurately mimic the complex structure of trabecular bone [1]. This study aimed to investigate the suitability of stereolithography (SLA) printing to produce synthetic trabecular bone models.

METHODS: The synthetic bone models were printed by SLA using a CAD-model generated from micro-computed tomography (micro-CT) synchrotron images of human trabecular bone [2]. To adjust the printing parameters, the influence of the following variables on the mechanical properties was investigated: printer type, orientation, resolution and UV-curing time. Subsequently, the trabecular CAD-model was printed at the original scale (scale factor 1), and with several enlarging factors. Mechanical properties were evaluated by compression and screw pullout tests, and structure replicability was assessed with micro-CT.

RESULTS & DISCUSSION: The elastic modulus of the control group was not statistically different from that of the other batches after the printing parameters configuration, standard parameters were therefore used. The orientation of the samples on the build platform of the printer did not seem to have an influence on the ratio Bone Volume/Total Volume for trabecular samples. For the bone models with scaling factors below 1.8, micro-CT image analysis showed major artefacts due to printing and a low accuracy in trabecular thickness distribution. Analysis of the total printed volume showed a difference to the original model higher than 50% for scale 1.5 and lower than 10% for scales 1.8 and above (Fig. 1). A refined overlap comparison with the original bone model showed that the scale 1.8 exhibited errors higher than 20%, implying printing inaccuracies of the smaller details. The pullout strength obtained for SLA-printed parts was higher than for existing synthetic models (Sawbones™) and cadaveric specimens, but within the same range as FDM-printed parts in poly (lactic acid) [2].

CAD-model Scale 4.3 Scale 1.8 Scale 1.5

Fig. 1: Volumetric comparison of the CAD-model (in grey) overlapped with the µCT-image dataset from the printed samples (extra material in purple).

CONCLUSIONS: Trabecular bone models with a scale factor of 1.8 or greater could be produced with acceptable accuracy but models with smaller scale factors were not well printed. Nevertheless, for the same 3D model, a higher resolution was reached by SLA as compared to FDM [2].

ACKNOWLEDGEMENTS: The authors are grateful to Adam Engberg at U-PRINT: Uppsala University's 3D-printing facility at the Disciplinary Domain of Medicine and Pharmacy for support and advice on the printers. This research was funded by Sweden's Innovation Agency VINNOVA, grant number 2019-00029.

REFERENCES: [1] M. Poukalova et al., "Pullout strength of suture anchors: Effect of mechanical properties of trabecular bone," J. Biomech., vol. 43, no. 6, pp. 1138–1145, Apr. 2010, doi: 10.1016/j.jbiomech.2009.12.007, [2] D. Wu, A. Spanou, A. Diez-Escudero, and C. Persson, "3D-printed PLA/HA composite structures as synthetic trabecular bone: A feasibility study using fused deposition modeling," J. Mech. Behav. Biomed. Mater., vol. 103, p. 103608, Mar. 2020, doi: 10.1016/j.jmbbm.2019.103608.

Success and Survival Rates of Immature Third Molar Autotransplantation. 6-month Observation Period

M. Lejnieks[1,2,3], I. Akota[1,2], G. Jakobsone[1,2], I. Salma[1,2,3], O. Radzins[1,2,3], L. Buss,[1,2,3], M. Lauskis[1,2,3]

[1]Riga Stradins University, Department of Oral and Maxillofacial Surgery, LV, [2]Riga Stradins University Institute of Stomatology, Latvia, [3]Baltic Biomaterials Centre of Excellence, Headquarters at Riga Technical University, Riga, LV

INTRODUCTION: Autotransplantation of third molars with unformed roots has several biological benefits, preservation and regeneration of bone, providing a functioning tooth. The aim of the study was to investigate the efficiency of autotransplantation of the immature third molars, performed in the Institute of Stomatology, Riga Stradins University.

METHODS: There were 22 patients (7 males and 15 females, mean age 17,9 years, range 14 - 22) with 26 immature third molars autotransplantations. Out of them in one patient tree teeth were transplanted. In two patients two teeth were transplanted. Only first transplanted tooth was included in research. Procedures were performed from 14/08/2019 till 03/08/2020 by the same specialist. Only patients with at least 6-month observation period were included.
Three teeth from the maxilla to the maxilla, eight teeth from the maxilla to the mandible, nine teeth from the mandible to the mandible and two from the mandible to the maxilla were transplanted.

Gingival pockets and vitality tests for transplanted teeth were assessed clinically. Bone attachment, obliteration of pulp chamber, root length growth and possible appearance of root resorption were evaluated in the periapical radiographs.

RESULTS: An increased gingival pocket of 6-8 mm was observed in two cases. Positive vitality test was assessed in 10 teeth, delayed response- in 6 teeth, no response in 6 teeth.
Radiological examination revealed reestablishment of the bone attachment in 20 teeth. Pulp chamber obliteration was observed in 13 teeth. Root continues to grow in length in 6 teeth. Internal root resorption was detected in 1 case.

DISCUSSION & CONCLUSIONS: Autotransplantation of the immature third molars could be considered as effective method for replacement of missing molars. Further development for method using 3D printed replicas and evaluation of long-term results is under way.

ACKNOWLEDGEMENTS: The authors acknowledge financial support from the European Union's Horizon 2020 research and innovation programme under the grant agreement No 857287.

Electrospun Fibrous Implant Sonocoated with Antibacterial and Osteoconductive Nanoparticles

J. Higuchi[1], A. Chodara[1,2], U. Szałaj[1,2], S. Dąbrowska[1,2], J. Wojnarowicz[1], W. Łojkowski[1]

[1]*Laboratory of Nanostructures, Institute of High Pressure Physics, Polish Academy of Sciences, Warsaw, PL*

[2] *Faculty of Materials Science and Engineering, Warsaw University of Technology, Warsaw, PL*

INTRODUCTION: The work addresses the reconstruction of bone tissue in dentistry. In particular, guided tissue regeneration (GTR) and guided bone regeneration (GBR). Both of these surgical methods involve the restoration of bone deficiencies by means of barrier membranes. They are critical for maintaining the space and restoration of lost tissues. Thus, approach considering both bone regeneration and epithelium separation should be considered when designing new barrier membrane construct [1]. Moreover, in dental surgery procedures the risk of bacterial infections is particularly high. Therefore, antibacterial properties of such membranes are highly demanded [2]. The main goal of the study was to obtain:

•Antibacterial properties caused by the presence of ZnO-based biocidal nanoparticles ultrasonically deposited on the fibrous structure.

•Osteoconductive properties due to the enhanced surface nanotopography and presence of calcium/phosphorus ions in the nanohydroxyapatite coating of the fibers.

METHODS: Membranes were electrospun from PDLLA/PLGA blend. After electrospinning, membranes were fixed and immersed in the vessel with nHA with the addition of ZnOAg nanoparticles suspended in aqueous medium. Ultrasonic waves were induced nearby material surface according to the method of ultrasonic coating [3,4]. As a result of the process, liquid jets were depositing the layers of nanoparticles on the surface of the fibers. The resulted fibers coated with NPs were tested against *Escherichia coli* and *Staphylococcus aureus* bacteria strains.

RESULTS: As a result of electrospinning of the polymer uniform porous structure was created. The sonocoating process induced nearby the textile substrate resulted in depositing nHA-ZnO and nHA-ZnOAg particles mixtures on fibers. SEM imaging revealed that nanoparticles covered fibres but did not interfere with the structure of the base material. The porosity of the fibrous mesh was maintained practically unchanged and wettability of the material was highly increased while the antibacterial agent was found to limit bacterial growth.

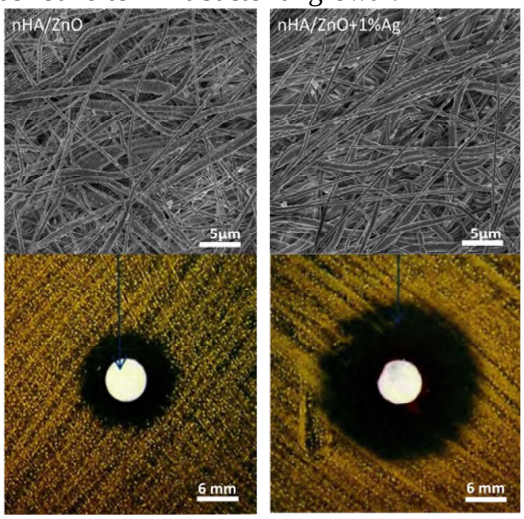

Fig. 1: SEM images of the obtained structures and inhibition zones on Staphylococcus aureus seeded agar plates.

DISCUSSION & CONCLUSIONS: The microbial invasion and biomaterial-centered infections remain a major problem that limits the performance of the materials. We successfully introduced antibacterial nanoparticles into the material structure. The obtained structure can serve as a promising biodegradable structure for GTR/GBR procedures with the combined osteoconductive/antibacterial function.

ACKNOWLEDGEMENTS: This work was financed by the Center for Preclinical Research and Technology - CePT II (RPMA.01.01.00-14-8476/17 – 01).

REFERENCES:

[1]V.Thomas, et al. Medicine.Curr. Nanosci.2006,2, 155–177. [2] Y.Gao, et al. J. of Applied Polymer Science, 131:18, 1-13. [3] Rogowska-Tylman et al. Journal of Materials Science and Engineering: C, 2019, 99, 669-684. [4] Higuchi J., et al, Nanomaterials 2019, 9, 1625.